

## COMMUNICATION

[View Article Online](#)  
[View Journal](#) | [View Issue](#)Cite this: *Nanoscale Adv.*, 2022, 4, 14Received 8th October 2021  
Accepted 18th November 2021

DOI: 10.1039/d1na00730k

[rsc.li/nanoscale-advances](https://rsc.li/nanoscale-advances)

## Red, green, and blue light-emitting carbon dots prepared from gallic acid for white light-emitting diode applications†

Menglin Chen,<sup>a</sup> Can Liu,<sup>ID</sup> \*<sup>ab</sup> Yulong An,<sup>ID</sup> <sup>a</sup> Yan Li,<sup>ID</sup> <sup>ab</sup> Yunwu Zheng,<sup>ID</sup> <sup>a</sup>  
Hao Tian,<sup>c</sup> Rui Shi,<sup>a</sup> Xiahong He<sup>a</sup> and Xu Lin<sup>ID</sup> \*<sup>ab</sup>

Red, green, and blue CDs were successfully prepared by a solvothermal method using gallic acid as the raw material. The distinct optical features of these CDs are based on the differences in the size of their  $sp^2$ -domains, which can be governed by reaction solvents.

Carbon dots (CDs) are widely used in biosensing, bioimaging, fluorescent labeling and other fields due to their good fluorescence properties and biocompatibility.<sup>1–3</sup> Compared with traditional fluorescent dyes, CDs have the advantages of a wide excitation range, strong fluorescence intensity, and good fluorescence stability.<sup>4,5</sup> There are also many methods for preparing CDs, such as oxidation, hydrothermal synthesis, and microwave synthesis.<sup>6,7</sup> Biomass has also been used to prepare CDs with excellent characteristics because it has many sources, is non-toxic and has renewable characteristics.<sup>8–10</sup>

To date, studies have used different solvents to develop multicolor wavelength-emitting CDs.<sup>11–13</sup> Recently, the mechanism of solvent discoloration has attracted attention.<sup>14,15</sup> The research and characterization results show that the reaction in different solvents will produce differently sized  $sp^2$ -domains of the prepared CDs, and the solvent not only acts as a reaction medium, but also as a reaction precursor, which affects the CDs. When preparing carbon dot materials with unique fluorescence properties, specific solvents can be used in the synthesis.<sup>16,17</sup>

CDs have been synthesized from many kinds of biomass materials. Aromatic hydrocarbons were selected as the carbon

source from among many precursor materials to obtain high-quality CDs. Gallic acid (GA) is a naturally derived polyphenolic compound with a benzene ring (Fig. 1) and is widely found in fruits and plants. Although its structure is very favorable for the preparation of CDs, multicolor luminescent CDs based on GA have not been reported because it is difficult to obtain an extended conjugated structure with only the phenolic hydroxyl group of GA.<sup>18–20</sup>

Herein, we report the preparation of multicolor luminescent CDs based on GA, which can react with *o*-phthalaldehyde *via* the aldol condensation reaction.<sup>21,22</sup> The high reactivity between the phenol hydroxyl group and benzaldehyde group can ensure the formation of a relatively large conjugated system in the process of CD formation, and promote the redshift of the fluorescence wavelength. By testing a variety of solvents, such as methanol, ethanol, acetone, octane, toluene, THF, and DMF, we found that GA and *o*-phthalaldehyde can produce stable CDs with orange-red emission under alkaline conditions with methanol as the solvent; the use of acetone as a solvent can result in stable CDs that emit green light. With the same precursor and under identical alkaline conditions, DMF was used as the solvent to

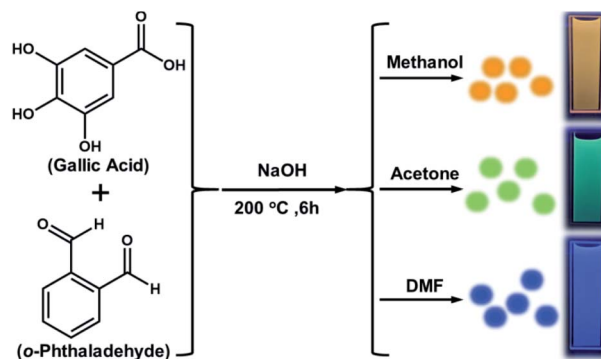


Fig. 1 Solvent engineering strategy for the synthesis of multicolor fluorescent CDs using gallic acid and *o*-phthalaldehyde as starting materials under alkaline conditions.

<sup>a</sup>Key Laboratory for Forest Resources Conservation and Utilization in the Southwest Mountains of China, Southwest Forestry University, Kunming, China. E-mail: [linxunefu@126.com](mailto:linxunefu@126.com)

<sup>b</sup>Key Laboratory of State Forestry Administration for Highly-Efficient Utilization of Forestry Biomass Resources in Southwest China, Southwest Forestry University, Kunming, China

<sup>c</sup>Agro-products Processing Research Institute, Yunnan Academy of Agricultural Sciences, Kunming, China

† Electronic supplementary information (ESI) available. See DOI: 10.1039/d1na00730k

prepare blue-emitting CDs. However, the fluorescence of the CDs prepared in ethanol, toluene, octane and THF was very weak (Fig. S1†). Three typical CD samples with blue (by DMF), green (by acetone), and red (by methanol) fluorescence were chosen for further characterization and were labelled B-CDs, G-CDs, and R-CDs, respectively. At the beginning of the experiment, the effects of (*o*-, *m*-, and *p*-) phthalaldehyde on the synthesis of CDs were also studied. It was found that the latter two compounds could not form fluorescent CDs when reacted with GA. The obtained RGB-CDs can be dispersed in various common organic solvents to obtain a clear solution. For example, clear RGB-emitting solutions were formed when the CDs were dispersed in ethanol under UV irradiation ( $\lambda_{\text{ex}} = 365$  nm; Fig. 1).

Transmission electron microscopy (TEM) was performed to examine the morphologies of the prepared CD samples. As shown in Fig. 2a–c, the TEM image shows that the R-CDs, G-CDs and B-CDs were monodisperse, and their sizes were 2.2 nm, 2.7 nm, and 2.9 nm, respectively. The high-resolution TEM images (Fig. 2d–f) of the samples show well-resolved lattice fringes of graphitic carbon with an interplanar spacing of 0.22 nm, similar to the (100) crystal plane of graphitic carbon.<sup>14</sup> Obviously, the similar particle size of the three samples suggests that the quantum size effect was not the dominant mechanism responsible for the chromatic emissions.<sup>23</sup>

The UV/Vis absorption spectra of the CDs were measured in ethanol, as shown in Fig. 3a. In the UV region, absorption peaks were observed at 254, 225, and 220 nm for R-CDs, G-CDs, and B-CDs, respectively; these peaks corresponded to the  $\pi$ - $\pi^*$  transitions of the C=C bonds in the carbon cores.<sup>24</sup> Moreover, typical B absorption bands (269 and 273 nm) were observed for G-CDs and B-CDs, indicating the retention of the isolated aromatic structure within the carbon cores. In contrast to the G-CD and B-CD spectra, the spectrum of the R-CDs did not have a B absorption band, which means that they had a longer conjugated structure. Unlike many other reported CDs,<sup>25</sup> ours did not exhibit surface-defect state absorption in the visible region. Fig. 3b–d shows the fluorescence emission (PL) spectra

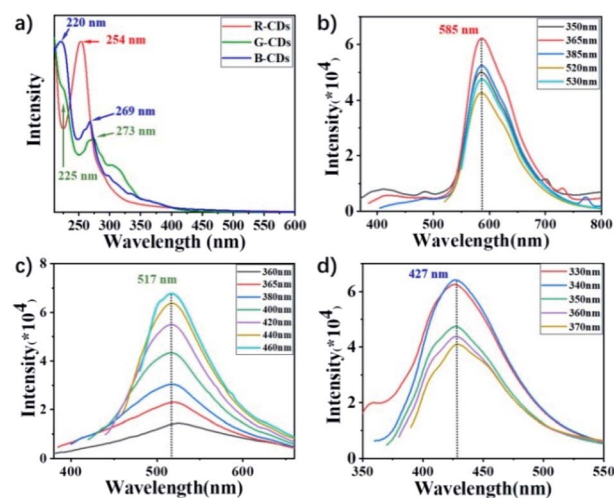


Fig. 3 (a) UV/Vis absorption spectra of R-CDs, G-CDs, and B-CDs ( $c = 0.1 \text{ mg mL}^{-1}$ ); (b–d) PL emission spectra of R-CDs, G-CDs, and B-CDs in ethanol at different excitation wavelengths ( $c = 0.1 \text{ mg mL}^{-1}$ ).

of three kinds of CDs in ethanol solution. The emission of R-CDs, G-CDs and B-CDs is almost independent of the excitation wavelength.<sup>26</sup> As seen in the corresponding fluorescence spectra, the R-CDs excited using 350–530 nm light showed a fluorescence peak at 585 nm, and a quantum yield of 23% was obtained under 500 nm excitation. For G-CDs, strong green emission was observed. Under excitation at 360–4460 nm, an emission band was formed at 517 nm, and a quantum yield of 11% was obtained under excitation at 500 nm. Additionally, B-CDs showed obvious blue light emission under UV excitation (330–370 nm), with a peak at 427 nm and a quantum yield of 10% under 340 nm excitation.

Fourier transform infrared (FT-IR) spectroscopy was performed to characterize the surface functional groups of the samples. As shown in Fig. 4a, the three CDs exhibited similar FTIR spectra, indicating that their chemical compositions were similar. According to the O–H stretching vibration near  $3437 \text{ cm}^{-1}$ , R-CDs, G-CDs and B-CDs have abundant hydrophilic groups, ensuring good solubility in polar organic solvents.<sup>25</sup> On the other bands corresponding to the functional groups, the peak at  $1625 \text{ cm}^{-1}$  is attributed to C=O, and the peak at  $1063 \text{ cm}^{-1}$  is attributed to C–O.<sup>23</sup> The Raman spectra of the three CDs (Fig. 4b) show two peaks at  $1348$  and  $1590 \text{ cm}^{-1}$ , corresponding to the disordered structures (D band) and the graphitic carbon domains (G band), respectively. The  $I_{\text{D}}/I_{\text{G}}$  ratios of the R-CDs, G-CDs, and B-CDs were 1.84, 2.07 and 2.19, respectively, indicating a gradual reduction in the size of the  $\text{sp}^2$ -domains.<sup>14</sup>

The functional groups of the three carbon dots were studied by X-ray photoelectron spectroscopy (XPS) to determine the group distribution characteristics of the prepared carbon dot samples. As shown in Fig. 4c, the elemental compositions of the different carbon dots were similar, and these CDs contained two main elements; the spectra show the C 1s core level ( $284.7 \text{ eV}$ ) and the O 1s ( $532.4 \text{ eV}$ ) core level.<sup>24</sup> The oxygen content of the G-CDs was the highest compared with those of the other two CDs (Table 1). In high-resolution X-ray photoelectron spectroscopy

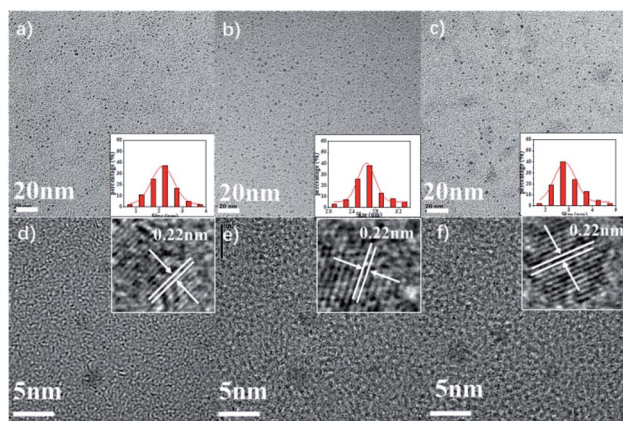


Fig. 2 (a–c) TEM images of R-CDs, G-CDs, and B-CDs. Inset: histograms and Gaussian fittings of the particle size distribution and (d–f) enlarged TEM images of R-CDs, G-CDs, and B-CDs.

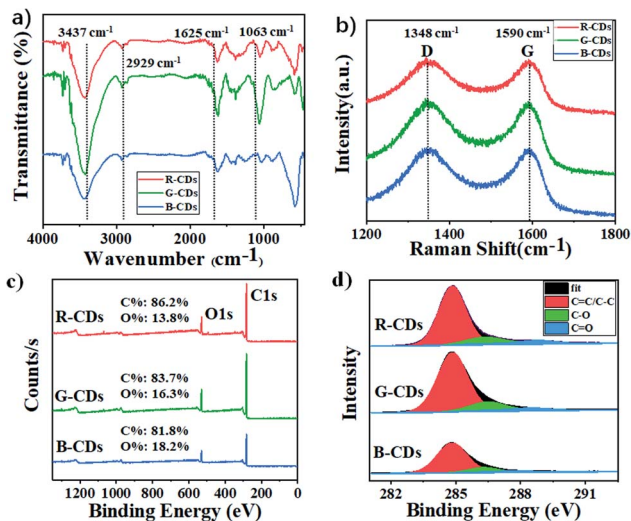


Fig. 4 (a) FT-IR spectra, (b) Raman spectra, (c) XPS survey spectra, and (d) high-resolution C 1s spectra of R-CDs, G-CDs, and B-CDs.

(Fig. 4d), the resolved C 1s spectrum shows peaks at 284.8, 286.4 and 288.2 eV, indicating the presence of the C=C/C-C, C-O and C=O bonds, respectively.<sup>26</sup> The proportion of the C=C/C-C components gradually decreases from R-CDs to G-CDs to B-CDs, indicating that the  $sp^2$ -carbon structure also decreases; this result is consistent with that of Raman spectroscopy.<sup>14</sup>

In general, there are two common CD photoluminescence mechanisms.<sup>23</sup> One is based on the band gap transition in the conjugated  $\pi$ -domains and the other is related to the surface-defects of the CDs. We believe that, in our system, the conjugated  $\pi$ -domains are the main factors controlling photoluminescence because none of our samples show absorption from surface-defects. This inference is also consistent with the results of Raman spectroscopy and XPS.

Furthermore, we discuss how the reaction solvent affected the synthesis of GA-based CDs. Through a time-dependent carbonization experiment, we found that the three carbon dots emit the same blue-green fluorescence in the early stage of the reaction, and their maximum emission wavelength is approximately 478 nm (Fig. S2†). As the reaction progressed, the maximum fluorescence wavelength of the G-CDs slowly red-shifted by approximately 40 nm and finally stopped at 517 nm (Fig. S2b†). In contrast, as the carbonization time increased, the maximum fluorescence wavelength of the B-CDs slowly blue-shifted by approximately 50 nm and finally fixed at 427 nm (Fig. S2c†). In contrast to the G-CDs and B-CDs, the R-CDs

showed two fluorescence centers, one at 427 nm, which is the same as that of B-CDs (Fig. S2a†). The other was at 585 nm, which is consistent with the final red fluorescence. As the reaction progressed, the fluorescence at 427 nm gradually decreased, while the fluorescence intensity at 585 nm gradually increased, and finally, only the fluorescence at 585 nm remained. From the above experimental results, it can be concluded that in the early stage of carbonization, the three samples produce fluorescent molecules with a similar structure through an aldol condensation reaction. Based on the comparison of fluorescence wavelengths (Fig. S3a†), these fluorescent molecules may contain an anthraquinone structure. As carbonization progresses, the reaction solvent plays a key role. The anthraquinone structure transforms into an anthracene structure in the B-CD core through a deoxidation reaction in DMF, which is also the reason why the fluorescence wavelength blue shifts with the progress of carbonization. For R-CDs, the reaction of deoxidation to form anthracene is also accompanied by a condensation reaction between the benzene rings under the action of ethanol, resulting in the expansion of the conjugated structure. The slowly expanding conjugated structure eventually contains the anthracene structure formed after carbonyl deoxidation, resulting in the disappearance of the fluorescence signal at 427 nm (Fig. S3b†). According to the XPS data, the G-CDs have the highest oxygen content, and the anthraquinone structure may be retained, but it is still uncertain what causes the subsequent redshift of approximately 40 nm. To determine the chemical structure in the carbonization process, we also carried out  $^1\text{H}$  NMR and  $^{13}\text{C}$  NMR characterization, but the spectrum was too complex for sufficient analysis. In short, we believe that the reaction solvent has little effect on the early aldol condensation reaction but plays an important role in the subsequent carbonization reaction, which also leads to the fluorescence color of these CDs (Fig. S4†).

To explore the optical and thermal stability of CD fluorescence, we studied its spectral changes at different visible and ultraviolet continuous irradiation times (Fig. S5†) and different temperatures (Fig. S6†). The results show that the maximum attenuation rate of the three carbon dots is less than 15%, and they have good optical and thermal stability (Fig. S7†).

These CDs can be used to make multi-color LEDs.<sup>27</sup> CDs/epoxy resin composites were plated on a purple LED chip to obtain R-LEDs, G-LEDs and B-LEDs (Fig. 5a–c). Their emission maxima were located at 585 nm, 510 nm and 425 nm, which were almost the same as those of the original CDs. The R-LEDs emitted a red light source (CIE coordinates  $x = 0.53$ ,  $y = 0.38$ ), the G-LEDs mainly emitted light in the green region (CIE coordinates  $x = 0.27$ ,  $y = 0.45$ ), and the B-LEDs emitted blue light (CIE coordinates  $x = 0.16$ ,  $y = 0.12$ ). Furthermore, we mixed the R-CDs, G-CDs and B-CDs in ethanol solution at a ratio of 1 : 2 : 2 (weight ratio) to obtain a white luminescent solution (Fig. 5d) and successfully prepared WLEDs using this ratio. The photoluminescence emission spectrum of the WLEDs prepared from the RGB-CD solution shows panchromatic emission at 400–700 nm, in which three different emission bands centered at 580 nm, 520 nm and 425 nm overlap, displaying CIE coordinates of (0.32, 0.34) (Fig. 5e and f).

Table 1 Elemental proportions and chemical bonds in RGB-CDs

	R-CD	G-CD	B-CD
C 1s	86.2%	83.7%	85.5%
O 1s	13.8%	16.3%	14.5%
C=C/C-C	86.3%	83.3%	80.5%
C-O	8.5%	13.3%	15.7%
C=O	5.2%	3.4%	3.8%





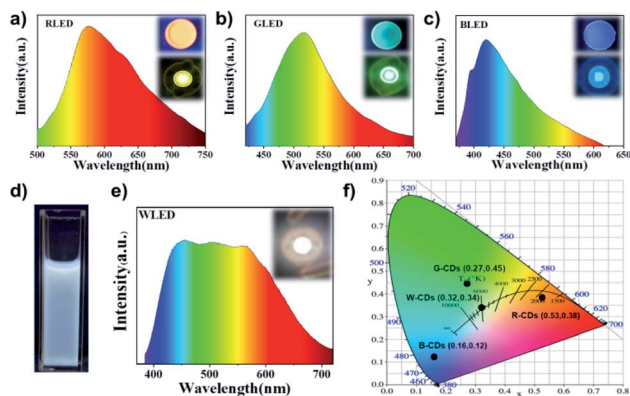


Fig. 5 (a–c) Emission spectra of RGB-LEDs operated at 3 V. Inset: Photograph of RGB-CD/epoxy resin films under 365 nm UV light and RGB-LED operated at 3 V. (d) Photograph of the prepared W-CD solution under UV light. (e) Emission spectra and photograph of the WLEDs operated at 3 V. (f) Calculated CIE coordinates from the photoluminescence spectra of the RGB-LEDs and W-CDs.

In summary, red, green, and blue luminescent CDs were prepared by a simple solvothermal reaction with gallic acid as the raw material. Participation of *o*-phthalaldehyde in the reaction may enlarge the conjugated structure and lead to a redshift of the emission wavelength of gallic acid-based CDs. We found that the choice of the reaction solvent is very important in this reaction because the solvents control the dehydration and carbonization processes of the precursors, determine the size of  $sp^2$ -conjugated domains and lead to different emission colors of the CDs. Our CDs can be dispersed into epoxy resin to form multicolor LEDs, including those that emit pure white light (CIE = 0.32, 0.34). We believe that our present study is expected to further the synthesis and application of natural polyphenolic-based CDs.

## Author contributions

Conceptualization, M. C. and C. L.; methodology, Y. A. and X. L.; writing—original draft preparation, M. C.; writing—review and editing, Y. L., Y. A. and Y. Z.; visualization, R. S.; supervision, H. T.; project administration, X. H.; funding acquisition, X. L. All authors have read and agreed to the published version of the manuscript.

## Conflicts of interest

The authors declare that the research was conducted in the absence of any commercial or financial relationships that could be construed as a potential conflict of interest. There are no conflicts to declare.

## Acknowledgements

This work was partially supported by the National Natural Science Foundation (No. 21961036), China Agriculture Research System (CARS-21), and the Applied Basic Research Programs of

Science and Technology Department of Yunnan Province (202101AT070041, 202002AA10007, 202102AE090042, and 2019ZG0901). The study also was supported by the Key Laboratory of State Forestry Administration for Highly-Efficient Utilization of Forestry Biomass Resources in Southwest China (2019-KF05).

## Notes and references

- 1 A. Li, Y. S. Yang, B. Y. Wang, J. B. Chang, Z. Y. Tang, B. Yang and S. Y. Lu, *Sci. Bull.*, 2020, **66**, 839–856.
- 2 S. Y. Lim, W. Shen and Z. Gao, *Chem. Soc. Rev.*, 2015, **44**, 362–381.
- 3 L. Cao, X. Wang, M. J. Meziani, F. Lu, H. Wang, P. G. Luo, Y. Lin, B. A. Harruff, L. M. Veca, D. Murray, S. Xie and Y. Sun, *J. Am. Chem. Soc.*, 2007, **129**, 11318–11319.
- 4 M. P. Han, K. Tang, Y. Wang, B. Lin and T. Cheng, *Nanoscale*, 2015, **7**, 1586–1595.
- 5 V. L. Colvin, M. C. Schlamp and A. P. Alivisatos, *Nature*, 1994, **370**, 354–357.
- 6 C. S. Woo, W. K. Bawendi and M. Bulovic, *Nature*, 2002, **420**, 800–803.
- 7 H. Du, W. Liu, M. Zhang, C. Si, X. Zhang and B. Li, *Carbohydr. Polym.*, 2019, **209**, 130–144.
- 8 X. Zhang, M. Jiang, N. Niu, Z. Chen, S. Li, S. Liu and J. Li, *ChemSusChem*, 2018, **11**, 11–24.
- 9 J. Shen, Y. Zhu, X. Yang and C. Li, *Chem. Commun.*, 2012, **48**, 3686–3699.
- 10 O. S. Wolfbeis, *Chem. Soc. Rev.*, 2015, **44**, 4743–4768.
- 11 X. Luo, C. Ma, Z. Chen, X. Zhang, N. Niu, J. Li, S. Liu and S. Li, *J. Mater. Chem. A*, 2019, **7**, 4002–4008.
- 12 T. Zhang, J. Zhu, Y. Zhai, H. Wang, X. Bai, B. Dong, H. Wang and H. Song, *Nanoscale*, 2017, **9**, 13042–13051.
- 13 K. Sato, R. Sato, Y. Iso and T. Isobe, *Chem. Commun.*, 2020, **56**, 2174–2177.
- 14 J. Zhan, B. Geng, K. Wu, G. Xu, L. Wang, R. Guo, B. Lei, F. Zheng, D. Pan and M. Wu, *Carbon*, 2018, **130**, 153–163.
- 15 J. Bai, Y. Ma, G. Yuan, X. Chen, J. Mei, L. Zhang and L. Ren, *J. Mater. Chem. C*, 2019, **7**, 9709–9718.
- 16 J. Zhan, B. Geng, K. Wu, G. Xu, L. Wang, R. Guo, B. Lei, F. Zheng, D. Pan and M. Wu, *Carbon*, 2018, **130**, 153–163.
- 17 S. Lu, L. Liu, H. Wang, W. Zhao, Z. Li, Z. Qu, J. Li, T. Sung, T. Wang and G. Sui, *J. Biomater. Sci.*, 2019, **7**, 2247.
- 18 P. Yang, X. Zhou, J. Zhang, J. Zhong, F. Zhu, X. Liu, Z. Gu and Y. Li, *Green Chem.*, 2021, **23**, 1834–1839.
- 19 S. K. Pal, M. Parashar, B. B. Kanrar, S. Panda, N. Roy, P. Paira and D. Panda, *J. Phys. Chem. C*, 2021, **125**(10), 5748–5759.
- 20 H. Hou, C. E. Banks, M. J. Jing, Y. Zhang and X. B. Ji, *Adv. Mater.*, 2015, **27**, 7861–7866.
- 21 S. T. Lu, L. P. Liu, H. N. Wang, W. C. Zhao, Z. Y. Li, Z. Qu, J. L. Li, T. D. Sun, T. Wang and G. C. Sui, *Biomater. Sci.*, 2019, **7**, 3258–3265.
- 22 H. Ding, S. B. Yu, J. S. Wei and H. M. Xiong, *ACS Nano*, 2016, **10**, 484–491.
- 23 J. J. Liu, D. W. Li, K. Zhang, M. X. H. Yang, C. Sun and B. Yang, *Small*, 2018, **14**, 1703919.



- 24 K. Jiang, S. Sun, L. Zhang, Y. Lu, A. Wu, C. Cai and H. Lin, *Angew. Chem.*, 2015, **127**, 5450–5453.
- 25 Y. Chen, H. Lian, Y. Wei, X. He, Y. Chen, B. Wang, Q. Zeng and J. Lin, *Nanoscale*, 2018, **10**, 6734–6743.
- 26 W. Meng, B. Wang, L. Ai, H. Song and S. Lu, *J. Colloid Interface Sci.*, 2021, **598**, 274–282.
- 27 Z. B. Wang, N. Z. Jiang, M. L. Liu, R. D. Zhang, F. Huang and D. Q. Chen, *Small*, 2021, 2104551.

